EMBO reports

EMBO open

scientific report

Structural basis of wedging the Golgi membrane by FAPP pleckstrin homology domains

Marc Lenoir[1], Ünal Coskun[2], Michal Grzybek[2], Xinwang Cao[2], Sabine B. Buschhorn[2], Jonathan James[1], Kai Simons[2] & Michael Overduin[1+]

[1]School of Cancer Sciences, University of Birmingham, Birmingham, UK, and [2]Max Planck Institute of Molecular Cell Biology and Genetics, Dresden, Germany

The mechanisms underlying Golgi targeting and vesiculation are unknown, although the responsible phosphatidylinositol 4-phosphate (PtdIns(4)P) ligand and four-phosphate-adaptor protein (FAPP) modules have been defined. The micelle-bound structure of the FAPP1 pleckstrin homology domain reveals how its prominent wedge independently tubulates Golgi membranes by leaflet penetration. Mutations compromising the exposed hydrophobicity of full-length FAPP2 abolish lipid monolayer binding and compression. The trafficking process begins with an electrostatic approach, phosphoinositide sampling and perpendicular penetration. Extensive protein contacts with PtdIns(4)P and neighbouring phospholipids reshape the bilayer and initiate tubulation through a conserved wedge with features shared by diverse protein modules.

Keywords: Golgi trafficking; membrane recognition; NMR spectroscopy; PH domain; phosphatidylinositol 4-phosphate

EMBO *reports* (2010) **11,** 279–284. doi:10.1038/embor.2010.28

INTRODUCTION

Our 303 pleckstrin homology (PH) domains generally bind to phosphoinositides (PIs) or proteins (Lemmon, 2008). Their functional assignment is compromised by our lack of solved structures of PH domains that bind to monophosphorylated PIs, or of other proteins in complex with phosphatidylinositol 4-phosphate (PtdIns(4)P), which is the most abundant monophosphorylated PI. This phospholipid is enriched in the *trans*-Golgi network (TGN) and recruits a family of four-phosphate-adaptor protein (FAPP)-related proteins through its PH domains (Levine & Munro, 2002; Wang *et al*, 2003; Sudhahar *et al*, 2008). These proteins move membrane components from tubular Golgi protrusions to the plasma membrane by reshaping the bilayer and working with Arf1 and PI 4-kinases (Levine & Munro, 2002; Godi *et al*, 2004; Vieira *et al*, 2005, 2006; D'Angelo *et al*, 2007).

The FAPP1 and FAPP2 proteins are closely related homologues that target the TGN by binding to PtdIns(4)P. They contain PH domains that are 88% identical, and FAPP2 also contains a glycolipid transfer protein-like domain (Lin *et al*, 2000; Godi *et al*, 2004). The principles that determine Golgi interactions by FAPP modules could apply to diverse PtdIns(4)P-binding proteins (Sudhahar *et al*, 2008). In mammalian cells, the FAPPs exemplify a set of Golgi-bound proteins, including ceramide transfer protein and oxysterol binding protein 1. Insights into their membrane recognition mechanism might illuminate the working of PtdIns(4)P-binding motifs in the distinct folds of adaptor protein AP-1 (Mills *et al*, 2003; Wang *et al*, 2003), Bem1p (Stahelin *et al*, 2007), EpsinR (Hirst *et al*, 2003), SdcA (Weber *et al*, 2006), SidC (Ragaz *et al*, 2008) and SidM (Brombacher *et al*, 2009), and might also shed light on how other cellular membranes are manipulated by the action of diverse protein modules, including BAR (Bin/Amphiphysin/Rvs) domains.

Here, we report nuclear magnetic resonance (NMR)-based solution structures of the free, micelle- and PtdIns(4)P-bound FAPP1-PH domain, the wedge of which is shown to be responsible for initiating membrane tubule formation. The basis of its multifarious lipid specificity and penetration into the bilayer leaflet is revealed, and the mechanism responsible for initiating membrane tubulation by PH domains is presented.

RESULTS AND DISCUSSION

The FAPP1-PH domain structure was solved by triple resonance NMR methods (Fig 1; supplementary Table S1 online), revealing a pronounced hydrophobic protrusion from the β1–β2 hairpin. The protrusion of the free state is encircled by an expansive

[1]School of Cancer Sciences, University of Birmingham, Henry Wellcome Building for Biomolecular NMR Spectroscopy, Vincent Drive, Edgbaston, Birmingham B15 2TT, UK
[2]Max Planck Institute of Molecular Cell Biology and Genetics, Pfotenhauerstrasse 108, Dresden 01307, Germany
[+]Corresponding author. Tel: +44 (0)121 414 3802; Fax: +44 (0)121 414 4486; E-mail: m.overduin@bham.ac.uk

Received 31 July 2009; revised 22 January 2010; accepted 3 February 2010; published online 19 March 2010

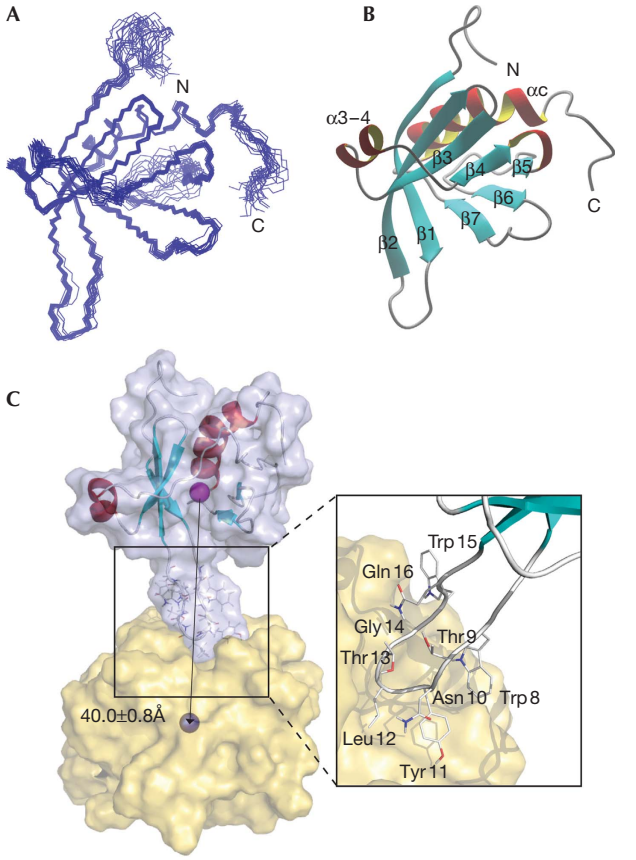

Fig 1 | Solution structures of FAPP1-PH determined by nuclear magnetic resonance and docked to a DPC micelle. (**A**) Backbone superposition of the 20 lowest energy structures and (**B**) ribbon of the representative structure with helices and β-strands labelled and coloured in aqua and red, respectively. (**C**) Structure of a representative FAPP1-PH micelle complex. The centre of the protein is depicted as a purple sphere, and the micelle surface and centre are coloured yellow and blue with the radius and distance from the protein indicated. The β1–β2 wedge inserts with an average distance of 8.3 Å between the micelle centre and deeply buried L12 $C_{\delta 2}$ group. The inset is rotated and expanded to show the interactions of the side chains with the DPC molecules. DPC, dodecylphosphocholine; FAPP, four-phosphate-adaptor protein; PH, pleckstrin homology.

basic surface (supplementary Fig S1 online) that does not bind detectably to inorganic phosphate, suggesting the need for a more specific partner (supplementary Fig S2 online). Interactions mediating membrane association were identified by adding micelles composed of dodecylphosphocholine (DPC) and CHAPS (3-[(3-cholamidopropyl)-dimethylammonia]-1-propane sulphonate). The entire β1–β2 loop showed chemical shift perturbations (CSPs), the largest of which occurred in the Trp 8, Thr 9 and Tyr 11–Trp 15 resonances (Fig 2A; supplementary Fig S3A,C online). Together with the dissociation constant (K_D) of 41.0 ± 4.6 μM, this suggests intimate encounters that position the nearby canonical PI pocket inside the interfacial zone of the membrane.

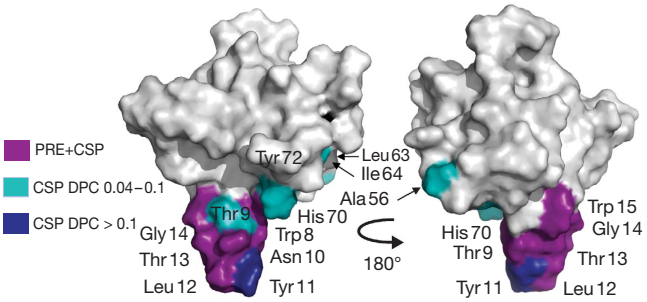

Fig 2 | Micelle insertion site mapped to the FAPP1-PH surface. The exposed FAPP1-PH β1–β2 loop residues exhibiting significant backbone or side-chain H_N PREs in the presence of micelles spiked with 14-doxyl phosphocholine as well as CSPs induced by DPC are indicated in purple. Those exhibiting medium or large chemical shift changes but undetectable or insignificant PREs are shown on the surface in aqua or blue, thus defining the region experiencing conformational changes on insertion. CSPs, chemical shift perturbations; DPC, dodecylphosphocholine; FAPP, four-phosphate-adaptor protein; PC, phosphocholine; PH, pleckstrin homology; PREs, paramagnetic relaxation enhancements.

The structure of the inserted state was modelled by using paramagnetic relaxation enhancements obtained by incorporating 5- and 14-doxyl spin-labelled phosphocholine into the micelle. The backbones of Thr 9, Asn 10, Tyr 11, Leu 12, Thr 13 and Gly 14 were inserted into the hydrophobic interior on the basis of NH signal broadening, as were the side chains of Trp 8, Asn 10, Trp 15 and Gln 16 (Fig 3; supplementary Fig S4 online). Together, this reveals an unprecedented burial of a wedge that spans residues Thr 9–Gly 16. The complexed structure was calculated by HADDOCK using 10 paramagnetic relaxation enhancement distance restraints, a flexible zone defined by the CSPs and refinement in water (Table 1; supplementary Table S3 online). The long axis of FAPP1-PH inserts at an angle of −159.26 ± 4.01 °, leaving the distal termini exposed. Together with an orthogonal twist of 251.74 ± 13.63 °, this defines the orientation of the protein on the micelle. The protein–micelle interface buries 914 ± 173 $Å^2$ and involves structural rearrangements in the penetrant β1–β2 loop (Fig 2; supplementary Table S3 online). An array of hydrogen bonding interactions are populated with 5–6 proximal DPC headgroups (Table 1). The Asn 10, Tyr 11 and Leu 12 side chains intercalate between the lipid acyl chains, whereas Trp 8 and Trp 15 buttress the interface.

The isolated FAPP1-PH domain was added to palmitoyl-oleoyl-phosphatidylcholine (POPC) membranes and was found to be necessary and sufficient to induce tubule formation when PtdIns(4)P was present (Fig 4A; supplementary Movie S1 online), recapitulating the PtdIns(4)P-dependent tubulation activity of full-length FAPP2 (Cao *et al*, 2009). In light of the assigned FAPP2 function, the Thr 11–Leu 12 wedge extremity in the conserved PH domain of full-length FAPP2 was mutated to GG and EE sequences to remove penetrant hydrophobic bulk and introduce repulsive force, respectively. The surface pressure assay involved injecting FAPP2 into monolayers composed of POPC and 2% PtdIns(4)P (Fig 4B). Insertion of wild-type protein increased the surface pressure until a critical concentration when lipid removal began, presumably reflecting a bilayer budding or reshaping process. The

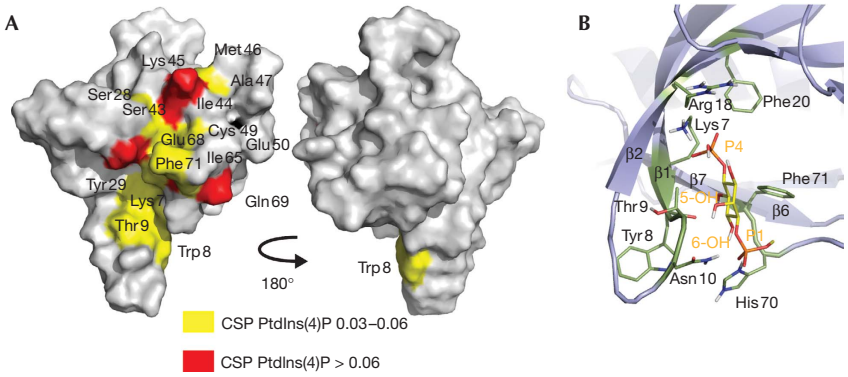

Fig 3 | PtdIns(4)P docking to the FAPP1-PH structure. (**A**) The PI binding pocket of the protein is coloured according to the extent of CSPs induced by the addition of an eightfold excess of C_6-PtdIns(4)P. (**B**) The docked headgroup and the hydrogen bonds are indicated in yellow and dashed lines, respectively. Ligand-binding residues are labelled and shown as sticks. CSPs, chemical shift perturbations; FAPP, four-phosphate-adaptor protein; PH, pleckstrin homology; PI, phosphoinositide.

Table 1 | Intermolecular restraints and interactions, which are present in at least 25% of the ensemble of structural models of FAPP1-PH docked with DPC micelles

Residue number	PRE	CSP	Hydrogen bonds	Hydrophobic contacts	
				Backbone	Side chain
Trp 8	NεH	0.06	0	0	8
Thr 9	*	0.08	5	0	7
Asn 10	NδH	0.03	5	0	7
Tyr 11	*	0.26	5	1	62
Leu 12	NH	0.37	0	11	85
Thr 13	NH	0.08	0	11	20
Gly 14	NH	0.08	0	8	0
Trp 15	NεH	0.16	0	8	0
Gln16	NεH	0.03	0	0	9

CSP, chemical shift perturbation; DPC, dodecylphosphocholine; FAPP, four-phosphate-adaptor protein; PH, pleckstrin homology.
*Paramagnetic relaxation enhancements could not be recorded owing to broadening of these resonances in the micelle complex.

GG mutant still interacted, but its insertion was compromised by an order of magnitude and no lipid removal was detected. As predicted, the EE mutation abolished binding, insertion and removal. Neither mutant full-length protein could tubulate the membrane sheets (supplementary Fig S5 online), indicating that membrane penetration by an intact wedge is required. We note that a number of mutations have been reported in human FAPP1-PH sequences by the Cancer Genome Anatomy Project, and these substitutions could affect various interactions and structural features; for example, the Y11D mutation would be predicted to impair membrane wedging and TGN traffic.

The ligand interactions of FAPP1-PH were mapped by NMR. A soluble form of PtdIns(4)P with dihexyl (C_6) chains binds to the free state in the fast exchange regime with an affinity in the μM–mM range, inducing CSPs across the canonical PI pocket (Fig 3A; supplementary Fig S3B,D online). Docking of the

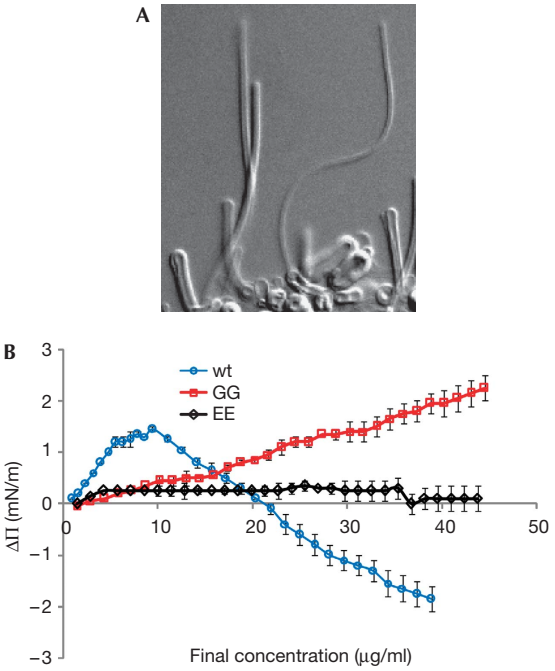

Fig 4 | FAPP-PH independently tubulates membrane sheets. (**A**) Membrane sheets composed of POPC and PtdIns(4)P (98:2 mol%) spontaneously formed dynamic ~10 μM-diameter tubules on injection of wild-type FAPP1-PH (1 mg/ml), as monitored in real time by differential interference contrast microscopy (supplementary Movie S1 online). (**B**) Surface pressure changes (ΔΠ) induced in POPC and PtdIns(4)P (98:2 mol%) lipid monolayers after injection of full-length FAPP2 with Thr 11–Leu 12 replaced with GG and EE sequences as well as wild-type protein at the concentrations indicated, with the latter control as described previously (Cao *et al*, 2009). The ΔΠ of the monolayer was recorded after protein injection into the subphase every 5 min. The isotherm was normalized to the initial established Π (~30 mN/m). FAPP, four-phosphate-adaptor protein; PH, pleckstrin homology; POPC, palmitoyl-oleoyl-phosphatidylcholine; PtdIns(4)P, phosphatidylinositol 4-phosphate; wt, wild type.

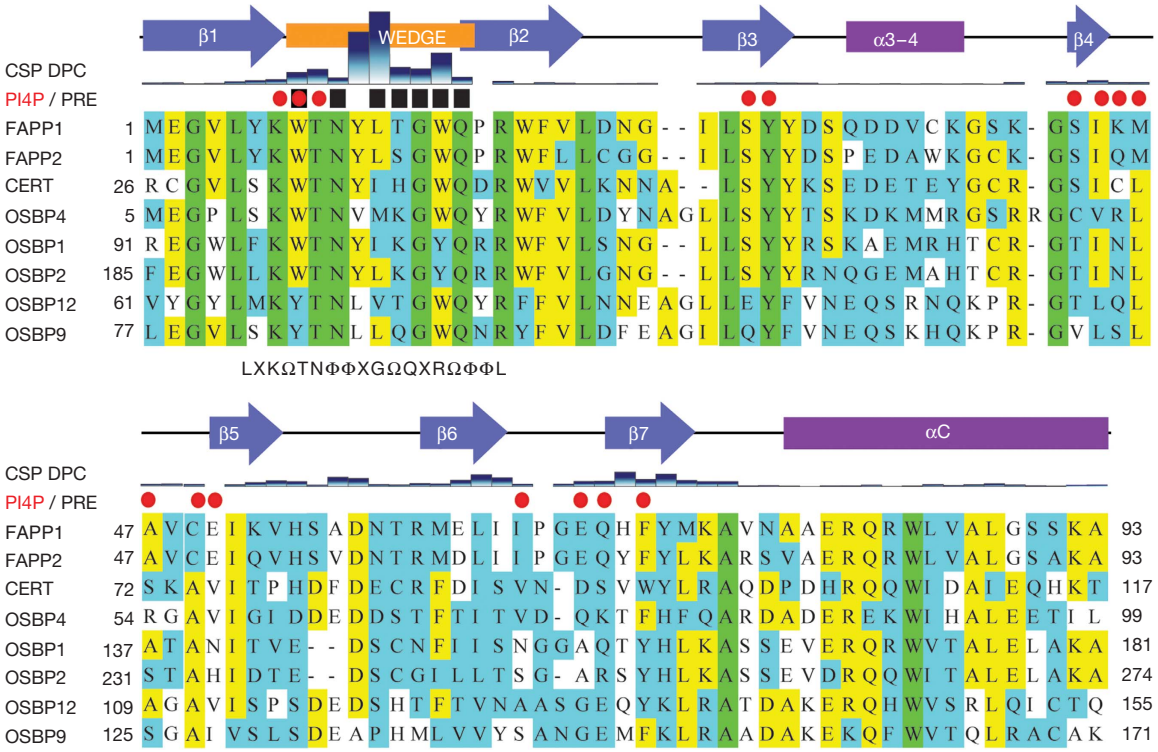

Fig 5 | Sequences alignment of FAPP-related PH domains with PtdIns(4)P binding activities. The FAPP1-PH secondary structures are shown; wedge residues are indicated under an orange bar, those with CSPs induced by PtdIns(4)P or exhibiting PREs are indicated by red dots and black squares, respectively. Most of the PtdIns(4)P and micelle contacts are mediated in residues in the consensus LXKΩTNΦΦXGΩQXRΩΦΦL motif in the β1–β2 loop, where X, Ω and Φ refer to any, aromatic and hydrophobic residues, respectively (Aasland *et al*, 2002). CERT, ceramide transfer protein; CSPs, chemical shift perturbations; DPC, dodecylphosphocholine; FAPP, four-phosphate-adaptor protein; OSBP, oxysterol-binding protein; PH, pleckstrin homology; PREs, paramagnetic relaxation enhancements.

headgroup based on NMR data (supplementary Table S4 online) helped to predict that the 4-phosphate is positioned by the Lys 7 residue, whereas the 1-phosphate orients near His 70 and Asn10. This facilitates parallel insertion of the β1–β2 loop and lipid acyl chains (Fig 3B). The 5- and 6-OH groups of the FAPP1-PH ligand were positioned by Trp 8, whereas the 2- and 3-OH groups abut Thr 9, Phe 20, Tyr 29 and Phe 71. Proximal residues including Arg 18 act to enhance the overall electropositivity that attracts the protein to acidic membranes.

FAPP1-PH does not bind exclusively to PtdIns(4)P. Soluble PtdIns(4,5)P_2 and PtdIns(3,5)P_2 also interact with the canonical PI binding site by the same assay, inducing large CSPs, especially in β7, that suggest a modified binding orientation and slightly higher affinity (supplementary Fig S6 online). However, this could simply reflect the greater attraction of polyphosphorylated PIs to the exposed basic surface in the absence of a bilayer context. Indeed, earlier studies show a twofold weaker association of FAPP1-PH with PtdIns(4,5)P_2 over PtdIns(4)P-containing vesicles, the latter of which are bound with a K_D of 230 nM (Stahelin *et al*, 2007). To explore further the electrostatic effects, acidic lipids including C_6-PtdSer were introduced and were found to stabilize insertion into PtdIns(4)P-containing micelles (supplementary Fig S7 online). The length of the PI chains also significantly affected the affinity, with the C_8-PtdIns(4)P/DPC micelles being bound by FAPP1-PH better by an order of magnitude than C_6-PtdIns(4)P/DPC micelles. Both stabilizations were evidenced by larger CSPs and by shifts of the interactions towards the slow exchange regime (supplementary Fig S3 online), indicating slower off rates. Other influences on TGN-localized activity of FAPPs include myristoylated Arf1, a cytosolic factor that interacts reversibly with the PH domain and membranes, thus influencing its GTPase activity and regulating PI 4-kinase (Levine & Munro, 2002; Godi *et al*, 2004).

Together, this suggests a model whereby the FAPP1-PH domain is recruited stepwise to the TGN by several concerted interactions. Nonspecific electrostatic attraction dips a wedge into the leaflet. This hydrophobic keel allows the protein to diffuse upright over the lipid bilayer, sampling PIs until PtdIns(4)P is recognized in the bilayer leaflet. This concentrates oriented FAPP molecules at PtdIns(4)P pools in the TGN, compressing the membrane and favouring local positive curvature. On reaching a critical protein concentration the bilayer buds spontaneously, yielding a tubule that grows rapidly. Although subsequent events such as tubule fission and vesicle delivery might rely on the recruitment of further factors, this defines the minimal machinery needed to initiate membrane tubulation at the TGN.

The wedge is highly conserved across the FAPP family of PH domains, including the ceramide transfer protein and oxysterol binding protein relatives, suggesting that they all tubulate the Golgi membrane by the same general mechanism (Fig 5).

Moreover, similar β1–β2 loop elements are found in other PH domains that target multiply phosphorylated PIs in other membranes (DiNitto & Lambright, 2006; Lemmon, 2007). Comparison with structures of the latter type reveals that the 4-phosphate orientation is maintained, although the 1-phosphate position is shifted to where it can be bound by their conserved (K/R)XR sequences. This motif is supplanted by a QXR motif in the FAPP family, which instead engages phosphocholine headgroups. In contrast to the parallel insertion of the PtdIns(4)P acyl chains and the inserted β1–β2 hairpin loop in FAPP1, a more perpendicular orientation of PtdIns(4,5)P_2, PtdIns(3,4)P_2 and PtdIns(3,4,5)P_3 headgroups is seen in crystal structures of other PH domains. Nonetheless, all of the PH domains of Akt, ARNO, DAPP1, dynamin, Grp1 and TAPP1 present exposed hydrophobicity at their β1–β2 hairpin tips, with flanking glycine and basic residues positioned to support analogous dynamic insertions into their plasma membrane destinations.

The PH wedge mechanism provides a basis for understanding diverse PtdIns(4)P-binding proteins. An exposed cluster of basic and hydrophobic residues is also presented by AP-1 for binding PtdIns(4)P in the Golgi membrane (Heldwein *et al*, 2004). The ENTH domain of the clathrin adaptor EpsinR instead utilizes an inducible amphipathic helix to bind PtdIns(4)P and insert into the Golgi membrane (Miller *et al*, 2007). Recently, *Legionella pneumophila* proteins were discovered to bind to PtdIns(4)P during host cell infection, and all three proteins—namely SdcA (Weber *et al*, 2006), SidC (Ragaz *et al*, 2008) and SidM (Brombacher *et al*, 2009)—possess largely helical domains that suggest unique functions. Analogous wedge motifs have also been proposed for proteins, including those with F-bar domains that interact with the plasma membrane (Wang *et al*, 2009). Thus, the FAPP mechanism might illuminate how diverse membrane surfaces are manipulated and possibly sensed by a range of different protein folds presenting hydrophobic wedges to insert into bilayers.

METHODS

Expression and purification. A human FAPP1-PH construct containing a C94S substitution was expressed in *Esherichia coli* by using a pGEX-6P-1 vector (Amersham Biosciences, Piscataway, NJ, USA) in M9 media supplemented with $^{15}NH_4Cl$ and $^{13}C_6$-glucose. The FAPP2 cDNA was subcloned into a pGEX-6P-1 vector (GE Healthcare, Little Chalfont, Buckinghamshire, UK) and point mutations were created by using the QuikChange XL kit (Stratagene, La Jolla, CA, USA). The sequences of all constructs were verified. The GST fusions were cleaved with PreScission protease (GE Healthcare) and purified over Superdex columns (GE Healthcare). The monomeric state was determined by analytical ultracentrifugation and NMR methods (supplementary Fig S8,S9 online) in the presence of 9.6 mM β-mercaptoethanol. The PH domain was exchanged into 20 mM Tris buffer, pH 7.0, and 100 mM NaCl, purified on a HiTrapQ column, concentrated, and NaN_3 (1 mM) and D_2O (10% v/v) were added.

NMR spectroscopy. The spectra of 100–500 μM uniformly ^{15}N or $^{15}N/^{13}C$-labelled protein were collected at 298 K on 600–900 MHz INOVA spectrometers (Varian Inc, Palo Alto, CA, USA). Pulse sequences used for assignment included HNCO, HNCA, HN(CO)CA, HNCACB, HN(CO)CACB, H(C)CH-TOCSY and CCH-TOCSY experiments. Interactions were monitored from the HSQC spectra of ^{15}N-labelled FAPP1-PH, and PtdIns(4)P (Cayman Chemical, Ann Arbor, MI, USA) was added at volumes from 100 μM to 2 mM. The micelles contained a 3:1 ratio of DPC (Anatrace, Santa Clara, CA, USA) and CHAPS (Sigma-Aldrich, Dorset, UK). The induced CSPs were calculated as $(\Delta\delta_H^2 + 0.15\Delta\delta_N^2)^{1/2}$. Distance restraints from 3D ^{15}N- and ^{13}C-edited nuclear Overhauser enhancement spectroscopy-heteronuclear single quantum coherence experiments were analysed by ARIA2.2 (Rieping *et al*, 2007). Slowly exchanging amides (supplementary Table S2 online) were deduced from the ^{15}N SOFAST-heteronuclear single quantum coherence (Schanda *et al*, 2005) spectra of protein dissolved in 99.96% D_2O. Backbone dihedral angles were deduced by using TALOS (Cornilescu *et al*, 1999). Paramagnetic relaxation enhancements were obtained by adding micelles spiked with equimolar 5- or 14-doxyl 1-palmitoyl-2-stearoyl-sn-glycero-phosphocholine (Avanti, Polar Lipids, Alabaster, AL, USA) to the ^{15}N-labelled PH domain (200 μM) and by standardizing NH intensities to those induced by spiking with unlabelled dipalmitoyl phosphocholine (Avanti, Polar Lipids).

Structural calculations. The conformational space of the FAPP1-PH structure was sampled by restrained Cartesian molecular dynamics, with 100 apo conformers being generated per iteration. The final set of structures were refined in explicit water, and the 20 lowest energy structures were selected and analysed with Crystallography and NMR System (Brunger *et al*, 1998). The PtdIns(4)P:PH complex was calculated using AUTODOCK4 (Morris *et al*, 1998; supplementary information online). The DPC:PH complex was calculated by HADDOCK (Dominguez *et al*, 2003; Dancea *et al*, 2008). A total of 10 paramagnetic relaxation enhancements restrained the distances between the micelle centre and the respective NH groups to 0–20 Å, with CSPs defining the flexible zone. The top 200 models were ranked according to their experimental energies, and statistics derived from the 20 best were reported.

Membrane sheet and monolayer assays. Membrane sheet tubulation and lipid monolayer surface pressure assays were performed as described previously (Cao *et al*, 2009). Droplets of mixed lipid stock solution consisting of POPC (Avanti Polar Lipids) and PtdIns(4)P (Matreya, Pleasant Gap, PA, USA) were spotted on coverslips, dried and rehydrated. A 5 μl solution of FAPP1-PH protein (1 mg/ml) was added and images recorded by DIC microscopy on a Zeiss Axioplan 2 microscope (Carl Zeiss Microimaging, Jena, Germany). Monolayer assays were performed by injecting a chloroform solution of POPC and PtdIns(4)P into the subphase, solvent evaporation and stepwise injection of the specified FAPP2 concentrations into the subphase after equilibration.

Supplementary information is available at *EMBO reports* online (http://www.emboreports.org).

ACKNOWLEDGEMENTS
We thank S. Whittaker and C. Ludwig for NMR acquisitions and discussions; The Henry Wellcome Building for Biomolecular NMR Spectroscopy and the European Network of Research Infrastructures for providing Access and Technological Advancements in bio-NMR for facility access; T. Dafforn and R. Parslow for biophysical data acquired through the support of the Biotechnology and Biological Sciences Research Council; and the European Union PRISM project for funding (to M.O. and K.S.).

CONFLICT OF INTEREST
The authors declare that they have no conflict of interest.

REFERENCES

Aasland R *et al* (2002) Normalization of nomenclature for peptide motifs as ligands of modular protein domains. *FEBS Lett* **513:** 141–144

Brombacher E, Urwyler S, Ragaz C, Weber SS, Kami K, Overduin M, Hilbi H (2009) Rab1 guanine nucleotide exchange factor SidM is a major phosphatidylinositol 4-phosphate-binding effector protein of *Legionella pneumophila*. *J Biol Chem* **284:** 4846–4856

Brunger AT *et al* (1998) Crystallography & NMR system: a new software suite for macromolecular structure determination. *Acta Crystallogr D Biol Crystallogr* **54:** 905–921

Cao X, Coskun U, Rossle M, Buschhorn SB, Grzybek M, Dafforn TR, Lenoir M, Overduin M, Simons K (2009) Golgi protein FAPP2 tubulates membranes. *Proc Natl Acad Sci USA* **106:** 21121–21125

Cornilescu G, Delaglio F, Bax A (1999) Protein backbone angle restraints from searching a database for chemical shift and sequence homology. *J Biomol NMR* **13:** 289–302

D'Angelo G *et al* (2007) Glycosphingolipid synthesis requires FAPP2 transfer of glucosylceramide. *Nature* **449:** 62–67

Dancea F, Kami K, Overduin M (2008) Lipid interaction networks of peripheral membrane proteins revealed by data-driven micelle docking. *Biophys J* **94:** 515–524

DiNitto JP, Lambright DG (2006) Membrane and juxtamembrane targeting by PH and PTB domains. *Biochim Biophys Acta* **1761:** 850–867

Dominguez C, Boelens R, Bonvin AM (2003) HADDOCK: a protein–protein docking approach based on biochemical or biophysical information. *J Am Chem Soc* **125:** 1731–1737

Godi A, Di Campli A, Konstantakopoulos A, Di Tullio G, Alessi DR, Kular GS, Daniele T, Marra P, Lucocq JM, De Matteis MA (2004) FAPPs control Golgi-to-cell-surface membrane traffic by binding to ARF and PtdIns(4)P. *Nat Cell Biol* **6:** 393–404

Heldwein EE, Macia E, Wang J, Yin HL, Kirchhausen T, Harrison SC (2004) Crystal structure of the clathrin adaptor protein 1 core. *Proc Natl Acad Sci USA* **101:** 14108–14113

Hirst J, Motley A, Harasaki K, Peak Chew SY, Robinson MS (2003) EpsinR: an ENTH domain-containing protein that interacts with AP-1. *Mol Biol Cell* **14:** 625–641

Lemmon MA (2007) Pleckstrin homology (PH) domains and phosphoinositides. *Biochem Soc Symp* **74:** 81–93

Lemmon MA (2008) Membrane recognition by phospholipid-binding domains. *Nat Rev Mol Cell Biol* **9:** 99–111

Levine TP, Munro S (2002) Targeting of Golgi-specific pleckstrin homology domains involves both PtdIns 4-kinase-dependent and -independent components. *Curr Biol* **12:** 695–704

Lin X, Mattjus P, Pike HM, Windebank AJ, Brown RE (2000) Cloning and expression of glycolipid transfer protein from bovine and porcine brain. *J Biol Chem* **275:** 5104–5110

Miller SE, Collins BM, McCoy AJ, Robinson MS, Owen DJ (2007) A SNARE-adaptor interaction is a new mode of cargo recognition in clathrin-coated vesicles. *Nature* **450:** 570–574

Mills IG, Praefcke GJ, Vallis Y, Peter BJ, Olesen LE, Gallop JL, Butler PJ, Evans PR, McMahon HT (2003) EpsinR: an AP1/clathrin interacting protein involved in vesicle trafficking. *J Cell Biol* **160:** 213–222

Morris GM, Goodsell DS, Halliday RS, Huey R, Hart WE, Belew RK, Olson AJ (1998) Automated docking using a Lamarckian genetic algorithm and an empirical binding free energy function. *J Comput Chem* **19:** 1639–1662

Ragaz C, Pietsch H, Urwyler S, Tiaden A, Weber SS, Hilbi H (2008) The *Legionella pneumophila* phosphatidylinositol-4 phosphate-binding type IV substrate SidC recruits endoplasmic reticulum vesicles to a replication-permissive vacuole. *Cell Microbiol* **10:** 2416–2433

Rieping W, Habeck M, Bardiaux B, Bernard A, Malliavin TE, Nilges M (2007) ARIA2: automated NOE assignment and data integration in NMR structure calculation. *Bioinformatics* **23:** 381–382

Schanda P, Kupce E, Brutscher B (2005) SOFAST-HMQC experiments for recording two-dimensional heteronuclear correlation spectra of proteins within a few seconds. *J Biomol NMR* **33:** 199–211

Stahelin RV, Karathanassis D, Murray D, Williams RL, Cho W (2007) Structural and membrane binding analysis of the Phox homology domain of Bem1p: basis of phosphatidylinositol 4-phosphate specificity. *J Biol Chem* **282:** 25737–25747

Sudhahar CG, Haney RM, Xue Y, Stahelin RV (2008) Cellular membranes and lipid-binding domains as attractive targets for drug development. *Curr Drug Targets* **9:** 603–613

Vieira OV, Verkade P, Manninen A, Simons K (2005) FAPP2 is involved in the transport of apical cargo in polarized MDCK cells. *J Cell Biol* **170:** 521–526

Vieira OV, Gaus K, Verkade P, Fullekrug J, Vaz WL, Simons K (2006) FAPP2, cilium formation, and compartmentalization of the apical membrane in polarized Madin-Darby canine kidney (MDCK) cells. *Proc Natl Acad Sci USA* **103:** 18556–18561

Wang YJ, Wang J, Sun HQ, Martinez M, Sun YX, Macia E, Kirchhausen T, Albanesi JP, Roth MG, Yin HL (2003) Phosphatidylinositol 4 phosphate regulates targeting of clathrin adaptor AP-1 complexes to the Golgi. *Cell* **114:** 299–310

Wang Q, Navarro MV, Peng G, Molinelli E, Lin Goh S, Judson BL, Rajashankar KR, Sondermann H (2009) Molecular mechanism of membrane constriction and tubulation mediated by the F-BAR protein Pacsin/Syndapin. *Proc Natl Acad Sci USA* **106:** 12700–12705

Weber SS, Ragaz C, Reus K, Nyfeler Y, Hilbi H (2006) *Legionella pneumophila* exploits PI(4)P to anchor secreted effector proteins to the replicative vacuole. *PLoS Pathog* **2:** 418–430